

Microstructure Evolution and Properties Improvement of Semi-solid Squeezed A356 Alloy During Heat Treatment

Tie Di¹, Yan Lufei¹, Guan Renguo¹, Ji Zhaoshan¹, Li Hongchao¹, Wang Xiang¹,
Liu Haifeng², Liu Debao³, Chen Minfang³

¹ Key Laboratory of Lightweight Structural Materials Liaoning Province, School of Materials Science and Engineering, Northeastern University, Shenyang 110819, China; ² The CITIC Dicastal Institute, Qinhuangdao 066011, China; ³ School of Materials Science and Engineering, Tianjin University of Technology, Tianjin 300384, China

Abstract: A356 alloy was processed by semi-solid squeeze casting followed by solution treatment at 540 °C. With increasing the solution time, Mg and Si elements dissolved into the matrix and led to solid solution strengthening. Results show that the tensile strength, elongation and hardness peak at 6 h and then decrease during solution treatment. Aging treatment at 180 °C for different time was carried out after solution treatment. With increasing the aging time, the fine spherical Mg₂Si phases are precipitated in the A356 alloy matrix, which are ~2 μm in size. The optimum heat treatment process is solid solution at 540 °C for 6 h followed by aging at 180 °C for 4 h. After solution and aging treatment, the tensile strength and elongation reach 336 MPa and 6.9%, respectively. Hardness reaches 1240 MPa after heat treatment, which is 106.7% higher than that of the cast alloy.

Key words: A356 alloy; semi-solid squeeze casting; heat treatment; microstructure; mechanical properties

Al-Si-Mg alloy can be easily heat-treated to gain adjustable mechanical properties. Due to its low density, favorable mechanical properties and good castability, Al-Si-Mg alloys are widely used in aviation, aerospace, automobile, machinery and many other industries^[1-4]. As a typical Al-Si alloy, A356 alloy consists of 7.00wt% Si, 0.43wt% Mg, 0.19wt% Fe, and balanced Al, which can be strengthened by heat treatment. Many researchers have studied the effect of alloy's composition, casting method and heat treatment method on microstructure of A356 alloy^[5-7].

The effects of solidification cooling rate on solid solution heat treatment of A356 alloy was studied by Yang^[8] et al. The results show that the high cooling rate of the solidification process can reduce the solid solution heat treatment time and improve the alloy tensile properties. Pramod^[9] et al found that after addition of Sc element and T6 heat treatment, the synthetic properties of the alloys can be improved significantly. Wu^[10] et al performed solution treat-

ment on A356 alloy with Al-5Sr-8Ce as a modifier, and successfully refined the microstructure and improved the tensile properties of the alloy. Elahi^[11] et al studied the effect of various cast and heat treatment conditions on impact ductility of A356 aluminum alloy, and proposed that the eutectic Si morphology is the main parameter to decide the mechanical behaviors of the alloy. Grain refinement and modification of Si morphology provide higher impact ductility after T6 heat treatment in regardless of the cast conditions. Wisutmethangoon^[12] et al studied the aged hardening effect of gas induced semi-solid process on A356 alloy, and proposed that the eutectic Si morphology is the main parameter to decide the mechanical behaviors of the alloy. The experimental results exhibit that the effects of aging time on tensile strength, yield intensity and elongation are significant, and these properties increase first and then decrease with increasing the aging time. Akhil^[13] et al demonstrated mechanical properties including impact strength,

Received date: March 12, 2020

Foundation item: National Key Research and Development Program of China (2018YFB2001800); National Natural Science Foundation of China (U1764254)

Corresponding author: Guan Renguo, Ph. D., Professor, School of Materials Science and Engineering, Northeastern University, Shenyang 110819, P. R. China, Tel: 0086-24-83691990, E-mail: guanrg@mail.neu.edu.cn

Copyright © 2021, Northwest Institute for Nonferrous Metal Research. Published by Science Press. All rights reserved.

ultimate tensile strength, and hardness after heat treatment can be improved according to section size. This is due to the further grain refinement effects in heat treatment. The effect of pre/post-T6-heat-treatment on the mechanical properties of laser welded semi-solid metal of cast A356 aluminium alloy was analyzed by Akhter^[14] et al. It is found that the fine dendrite structure of the weld metal contributes to the mechanical properties of the joint. The mechanical properties of the post-heat-treatment samples are higher than those of the pre-heat-treatment samples and as-cast materials. Zhu^[15] et al revealed that the values of mean diameter, roundness, and ratio of eutectic silicon particles decrease, while the tensile properties increase after T6 heat treatment. These effects are attributed to the decrease of secondary dendrite arm spacing, spheroidization of fine eutectic Si and precipitation hardening. Most of previous researches on the heat treatment of A356 alloy were based on the traditional casting processes. Tie^[16] studied the microstructure and mechanical properties of A356 alloy fabricated by semi-solid squeeze casting with vibrating tilt system. Based on that study, the heat treatment effect on microstructure and mechanical properties of A356 alloy manufactured by semi-solid squeeze castings was studied. The heat treatment process was optimized and the strengthening mechanism of heat treatment was revealed. The synthetical mechanical properties of A356 alloys fabricated by semi-solid squeeze casting were further improved.

1 Experiment

The experimental material was commercial A356 alloy whose main chemical composition is 7.00wt% Si, 0.43wt% Mg, 0.19wt% Fe, and balanced Al. The A356 alloy samples were manufactured by a rheological squeeze casting equipment developed by our team^[16]. The processing parameters were as follows: the casting temperature was 685 °C and the casting speed was 0.052 m/s. The casting temperature was within the semi-solid temperature range of A356 alloy. When the melt touched the surface of the device, the melt was subjected to a shearing stress and cooled rapidly. Therefore, the heterogeneous nucleation was generated on the surface of the sloping plate. Under the coupling field of vibration and shear, the nucleus continuously fell off from the plate, leading to grain spheroidization and grain refinement during the rapid solidification. The alloy was solid solution treated and aged in an electric furnace (DFHG-0-5 type, DF Tech, China). The samples were cooled by water after solid solution, and cooled by air after aging. The heat treatment process conditions are shown in Table 1.

After heat treatment, the sample was coarsely ground and mechanically polished, and then rinsed with alcohol. The 0.5vol% HF solution was used to corrode the sample for 50 s.

Table 1 Heat treatment conditions of the alloy

| Treatment | Solid solution | Aging |
|----------------|---------------------|-----------------|
| Temperature/°C | 540±5 | 180±5 |
| Time/h | 0.5, 2, 4, 6, 8, 12 | 0.5, 2, 4, 6, 8 |
| Cooling medium | Water | Air |

The sample was rinsed immediately with clean water and then with alcohol again. An OLYMPUS-DSX-500 metallographic microscope was used to observe the microstructure under different process conditions. The morphologies of grain and eutectic silicon of the alloy were observed. The roundness and average diameter of the grain were calculated by Eq.(1) and Eq.(2).

$$S_F = \frac{L_p^2}{4\pi A} \quad (1)$$

$$d = \frac{L_T}{N} \quad (2)$$

where S_F is the grain roundness, L_p is perimeter of the grain cross section, A is the grain sectional area, d is grain average diameter, L_T is measuring total line length, and N is the number of grains passed through the measuring line.

The precipitates in the alloy were observed by a scanning electron microscope (SEM, Japanese electronic JSM-7001F), and their chemical composition and distribution were analyzed by an energy dispersive spectroscopy (EDS). An electronic tensile testing machine (CMT5305; MST, China) was used to test the mechanical properties of the alloy sheets, and the tensile speed was set as 3 mm/min. The hardness value of the alloy was measured by a Vickers hardness tester (450SVD; Wolpert, USA). The applied load was 49 N and the holding time was 15 s. The fracture surface of tensile test samples was also observed by SEM to analyze the fracture mechanism. All the tests were carried out on five duplicates, and the data were expressed as mean±standard deviation (SD).

2 Results and Discussion

The microstructure of A356 alloy produced by semi-solid squeeze casting under different solution time at 540 °C is shown in Fig.1. The images depict that the Si particles in the eutectic phase are mainly of needle shape and the distribution is not homogeneous. After 0.5 and 2 h solution treatment, the tip of needle-like eutectic Si particles gradually separates from each other. At higher temperature, the Si atoms at the dendrites disperse and dissolve in matrix. The fusion of the eutectic Si is observed with the decrease of dendrites. The SEM image of A356 alloy produced by semi-solid squeeze casting and solution treatment at 540 °C for 6 h is shown in Fig.2. After 6 h, the eutectic Si further fuses and the stripe-like particles disappear. Eutectic Si particles gradually transform to the spherical shape, because the distribution of eutectic Si becomes more homogeneous. The refinement and

spheroidization of eutectic Si can significantly improve the alloy's mechanical properties, especially elongation, because the coarse Si particles can accelerate crack propagation rate and reduce the elongation of alloy^[17]. When the solid solution time is 8 and 12 h, the eutectic Si particles grow up to be coarse and inhomogeneous. With increasing the solid solution time from 0.5 h to 6 h, the average size of the Si particles in the eutectic phase decreases, and the morphology changes from needle-like shape to sphere. When the solid solution time is prolonged to more than 6 h, the Si particles size become coarse again, which leads to the decrease of mechanical properties. During the process of solid solution treatment, the morphology of Si particles can be classified as three stages: fusion of eutectic Si in needle-like shape, granulation of eutectic Si, and the coarsening of eutectic Si.

It can be concluded that the tensile strength, elongation and hardness of the cast alloy increase when the solution time changes from 0 h to 6 h (Fig.3). When the solid solution holding time is 6 h, the mechanical properties reach peak value. The tensile strength reaches 262 MPa, and the elongation reaches 16.7% with the hardness value of 910 MPa. With the further prolongation of solution time, the tensile strength, elongation and hardness all decrease. During solution treatment, Mg and Si elements dissolve into Al matrix, and the formation of supersaturated solid solution leads to solid solution

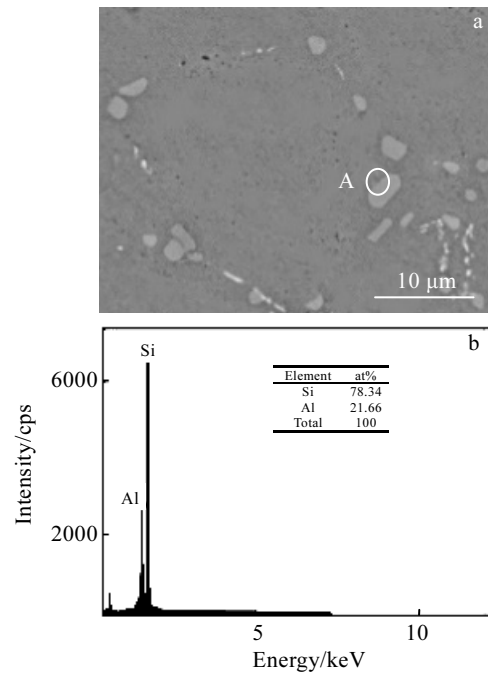


Fig.2 SEM image (a) and EDS result of position A in Fig.2a (b) of the alloy after solution treatment at 540 °C for 6 h

strengthening. The morphology of eutectic Si changes from needle-like shape to sphere at the initial stage of solution treatment. Spherical Si particles commonly avoid the split effects induced by the strip particles, therefore, improving the ductility of the alloy^[9]. The results show that when the holding time exceeds 6 h, the eutectic Si particles grow bigger, which leads to decrease of the mechanical properties.

The SEM fracture graphs of the A356 alloy at 540 °C for different solution time are presented in Fig.4. The fracture morphology of the untreated alloy shows a curved tearing edge. When the solid solution time is 2 h, the number of thick tearing edges on the section reduces

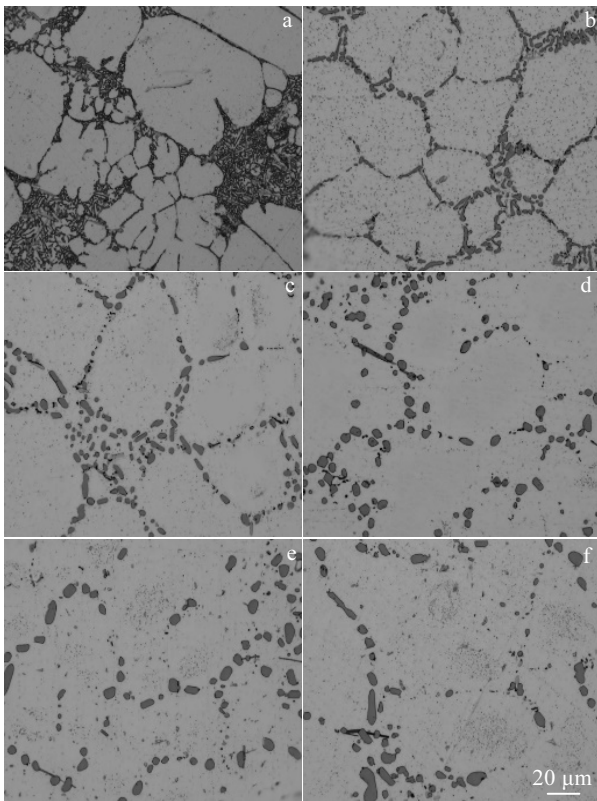


Fig.1 Microstructures of the alloy at 540 °C for different solution time: (a) 0 h, (b) 0.5 h, (c) 2 h, (d) 6 h, (e) 8 h, and (f) 12 h

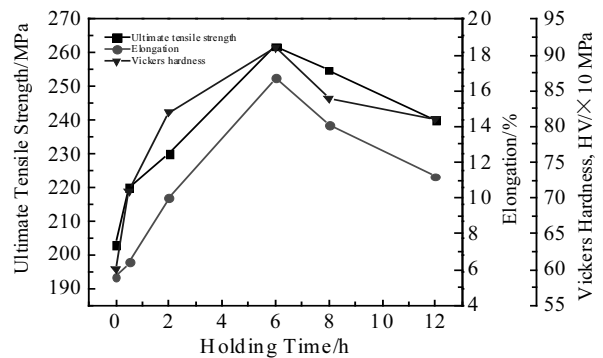


Fig.3 Variation of tensile strength, elongation and Vickers hardness at 540 °C for different solution time

while many smaller dimples are generated. When the solution time is 6 h, the dimples in the fracture surface are larger and deeper, and their distribution becomes inhomogeneous. Most of the dimples are equiaxed and formed by material internal separation. Due to the sliding effect, the vacancies gradually grow bigger and connect with other vacancies to form the dimple morphology^[7]. The dimple fracture is a typical plastic fracture, which indicates that the ductility of the alloy peaks when the solution time is 6 h. When the solution time extends to 12 h, the dimples in the fracture surface become larger and shallower, indicating the decrease of alloy ductility.

With increasing the aging time from 2 h to 6 h, the morphology and size of the eutectic Si particles in the A356 alloy do not change much (Fig.5). When the aging time increases to 8 h, the average size of eutectic Si particles grows from $\sim 2.0 \mu\text{m}$ to $2.5 \mu\text{m}$. The eutectic Si particles are mainly spherical after 4 h aging, and the spherical Mg_2Si precipitation is distributed among the Si particles (Fig.6). The supersaturated alloy matrix is in an unstable state, and shows a tendency of spontaneous decomposition^[18]. In the early stage of artificial aging, high supersaturation and vacancy concentration form the GP area (Fig.6c~6e). The GP area can provide heterogeneous nucleation for the formation of precipitation of strengthening phase during the aging process, which generates small-sized Mg_2Si precipitation to strengthen the matrix^[9].

During aging treatment, the tensile strength and hardness of the aged alloy first increase and then decrease, whilst the elongation decreases all the time (Fig.7). When the aging time increases from 0 h to 0.5 h, the tensile strength, elongation and hardness of the alloy do not

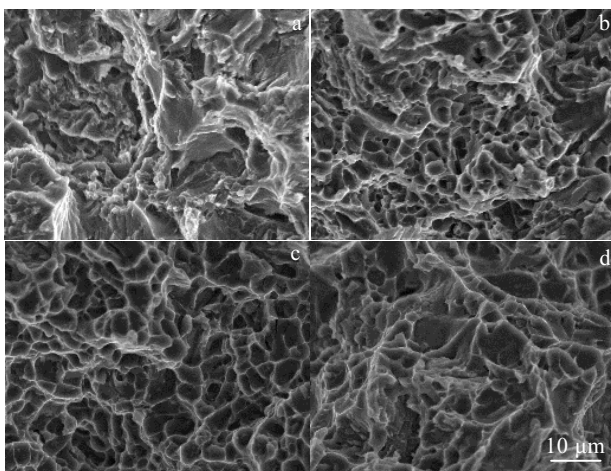


Fig.4 SEM fracture morphologies of solution treated alloys at $540 \text{ }^\circ\text{C}$ for different time: (a) untreated, (b) 2 h, (c) 6 h, and (d) 12 h

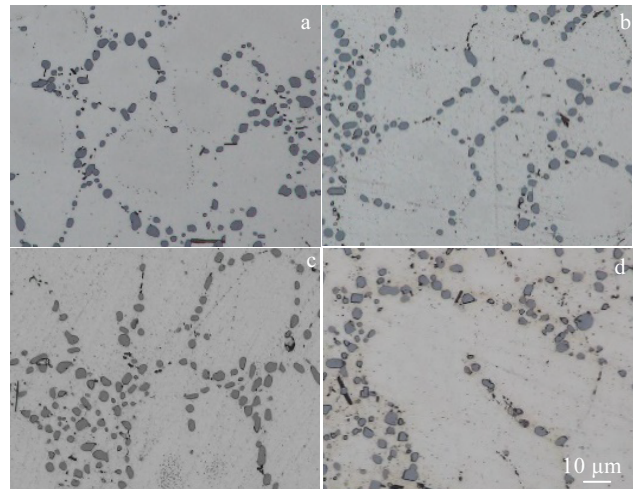


Fig.5 Microstructures of A356 alloy after aging at $180 \text{ }^\circ\text{C}$ for different time: (a) 2 h, (b) 4 h, (c) 6 h, and (d) 8 h

change significantly because few precipitations are generated. When the aging time further extends to 4 h, the tensile strength, hardness value and elongation reach 336 MPa, 1240 MPa and 6.9%, respectively. When the aging time is 8 h, the mechanical properties of the alloy peak and decrease with longer aging time. The supersaturated solid solution in the A356 alloy spontaneously decomposes at $180 \text{ }^\circ\text{C}$, and the solute atoms are diffused, accelerating to form the short-range ordered solute atomic enrichment area or atomic clusters (GP area)^[18].

When the aging time is shorter, the precipitates are mainly distributed in the GP area. Because the GP area is completely coherent with the matrix, its strengthening effect is not significant at this stage^[16]. With increasing the aging time, the GP area provides heterogeneous nucleation for the formation of precipitates. Mg_2Si is difficult to deform due to its high hardness, therefore, hindering the dislocation slip^[19]. When the volume fraction and size of the precipitates gradually increase, the strengthening effect on the alloy is further enhanced. As a result, with further increasing the aging time, the precipitates and the matrix become completely non-coherent^[7]. Then the volume fraction of the precipitation phases no longer increases while their size still grows, resulting in the strength declining^[9]. Considering the various factors, the optimum process parameters for the optimum mechanical properties are solution at $540 \text{ }^\circ\text{C}$ for 6 h and aging at $180 \text{ }^\circ\text{C}$ for 4 h. The hardness value of the aged alloy is 1240 MPa, which increases by 106.7% compared with the untreated alloy (Fig.8). The tensile strength is 336 MPa and the elongation is 6.9% after aging, which increases by 65.5% and 23.2%, respectively (Fig.8).

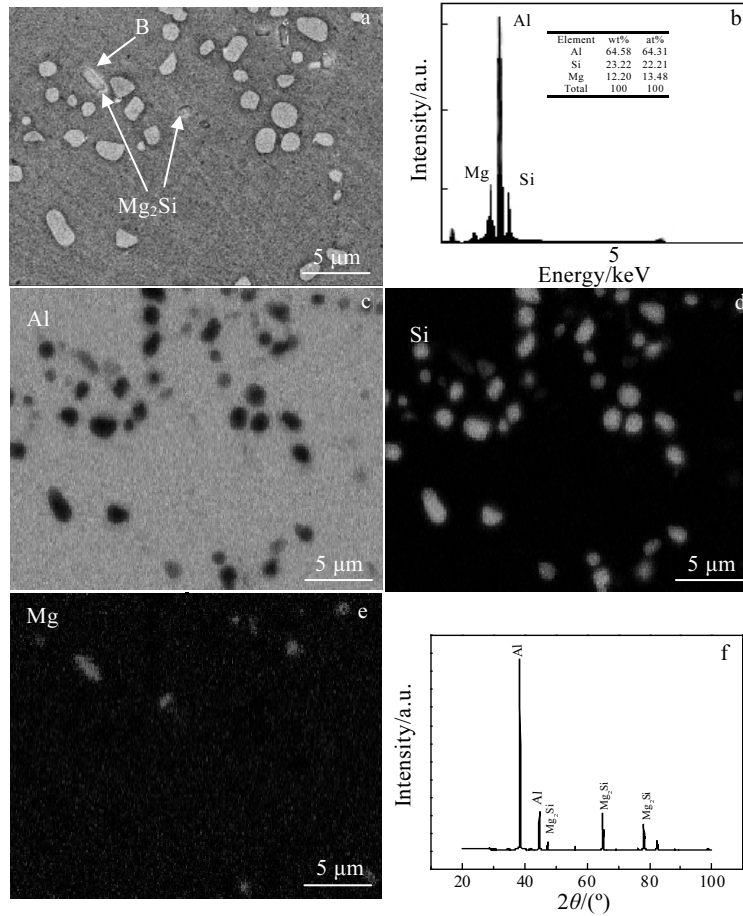


Fig.6 SEM image (a); EDS result of position B in Fig.6a (b); distributions of element Al (c), Si (d), Mg (e); XRD pattern (f) of the alloy aged at 180 °C for 4 h

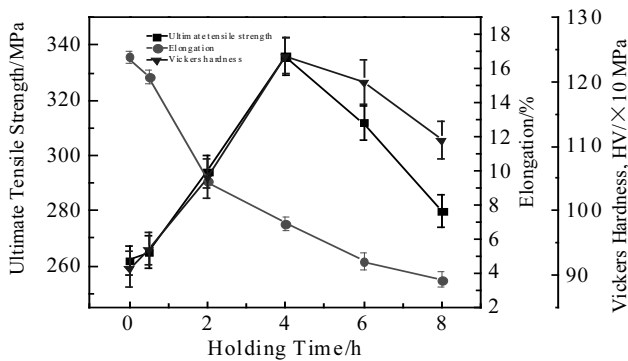


Fig.7 Variation of tensile strength, elongation and Vickers hardness of alloy aging treated at 180 °C for different time

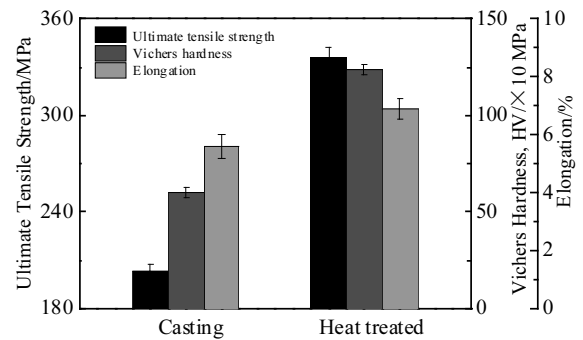


Fig.8 Tensile strength, elongation and hardness of the alloy before and after heat treatment

The SEM fracture morphology of the A356 alloy at 180 °C for different aging time are shown in Fig.9. Compared with the only-solution-treated alloy (Fig.9a),

the number of dimples in the fracture surface gradually reduces and the dimples are shallower after aging treatment. When the aging time is 4 h, the curved tearing edges are found on the fracture surface. When aging time

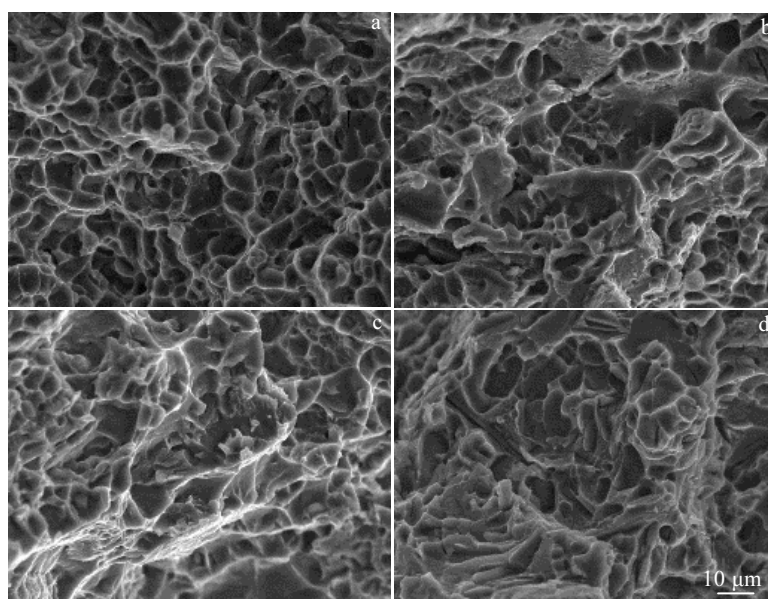


Fig.9 SEM fracture morphologies of alloy after different heat treatments: (a) solution for 6 h; (b) solution for 6 h and aging for 2 h; (c) solution for 6 h and aging for 4 h; (d) solution for 6 h and aging for 8 h

extends to 8 h, flat dissociation surfaces are observed, indicating that the fracture mode is quasi-cleavage crack. This is mainly due to the brittle precipitated Mg_2Si phases in the Al matrix after aging treatment^[7]. The strengthening phases and the matrix are completely non-coherent, so their deformation behavior is different. In the process of stress loading, stress concentration occurs around the precipitates, which leads to tearing^[20]. These fracture morphologies also reflect the mechanical property changes of the alloy.

3 Conclusions

1) During solution treatment, the eutectic Si particles dissolve into Al matrix and the stripe-like Si particles disappear. Eutectic Si particles gradually transform to the spherical shape, because the eutectic Si distribution becomes homogeneous. The refinement and spheroidization of the microstructure significantly improve the alloy's mechanical properties, especially elongation.

2) During aging treatment, the fine spherical Mg_2Si phases are precipitated in the A356 alloy matrix, which are $\sim 2 \mu m$ in size. With increasing the aging time, the precipitates and the matrix become completely non-coherent, leading to more significant strengthening effect.

3) The optimum heat treatment process is solid solution at $540^\circ C$ for 6 h followed by aging at $180^\circ C$ for 4 h. After solution and aging treatment, tensile strength and elongation reach 336 MPa and 6.9%, respectively. Hardness reaches 1240 MPa after heat treatment, which is 106.7% higher than that of the cast alloy.

References

- 1 Das P, Bhuniya B, Samanta S K *et al.* *Journal of Materials Processing Technology*[J], 2019, 271: 293
- 2 Yu W, He H, Zhang W *et al.* *Journal of Alloys and Compounds*[J], 2020, 814: 152 277
- 3 Ding H P, Tao Z T, Liu S *et al.* *Scientific Reports*[J], 2015, 5(1): 18 129
- 4 Chen R, Shi Y F, Qing-Yan X U *et al.* *Transactions of Nonferrous Metals Society of China*[J], 2014, 24(6): 1645
- 5 Ma Z, Zhang H R, Zhang X L *et al.* *Journal of Alloys and Compounds*[J], 2019, 803: 1141
- 6 Kund N K, Dutta P. *Journal of the Taiwan Institute of Chemical Engineers*[J], 2015, 51: 159
- 7 Madanat M, Liu M, Banhart J. *Acta Materialia*[J], 2018, 159: 163
- 8 Yang C L, Li Y B, Dang B *et al.* *Transactions of Nonferrous Metals Society of China*[J], 2015, 25(10): 3189
- 9 Pramod S L, Rao A K P, Murty B S *et al.* *Materials Science and Engineering A*[J], 2016, 674: 438
- 10 Wu D Y, Kang J, Feng Z H *et al.* *Journal of Alloys and Compounds*[J], 2019, 791: 628
- 11 Elahi M A, Shabestari S G. *Transactions of Nonferrous Metals Society of China*[J], 2016, 26(4): 956
- 12 Wisutmethangoon S, Thongjan S, Mahathaninwong N *et al.* *Materials Science and Engineering A*[J], 2012, 532: 610
- 13 Akhil K T, Arul S, Sellamuthu R. *Procedia Engineering*[J], 2014, 97: 1676
- 14 Akhter R, Ivanchev L, Burger H P. *Materials Science and Engineering A*[J], 2007, 447(1-2): 192

- 15 Zhu M, Jian Z Y, Yang G C et al. *Materials and Design*[J], 2012, 36: 243
- 16 Tie D, Wang Y, Wang X et al. *Materials*[J], 2020, 13(4): 845
- 17 Wang Q G. *Metallurgical and Materials Transactions A*[J], 2003, 34(12): 2887
- 18 Buchanan K, Colas K, Ribis J et al. *Acta Materialia*[J], 2017, 132: 209
- 19 Ma G H, Li R D, Li R X et al. *Materials Science and Engineering A*[J], 2016, 674: 666
- 20 Qian L, Toda H, Nishido S et al. *Acta Materialia*[J], 2006, 54(18): 4881

半固态挤压铸造 A356 合金在热处理过程中的组织和性能演化

铁 镒¹, 颜路飞¹, 管仁国¹, 季兆山¹, 李洪超¹, 王 祥¹, 刘海峰², 刘德宝³, 陈民芳³

(1. 东北大学 材料科学与工程学院 辽宁省轻量化用关键金属结构材料重点实验室, 辽宁 沈阳 110819)

(2. 中信戴卡研究院, 河北 秦皇岛 066011)

(3. 天津理工大学 材料科学与工程学院, 天津 300384)

摘 要: 半固态挤压铸造的 A356 合金首先在 540 °C 下进行固溶处理, 随着固溶温度升高, Mg 和 Si 原子逐渐溶解于基体中, 并产生了固溶强化作用。抗拉强度、延伸率和硬度在固溶 6 h 达到峰值, 之后合金力学性能随固溶时间延长而下降。在固溶处理之后合金在 180 °C 下进行了不同时间的时效处理。随着时效时间延长, Mg₂Si 相逐渐在基体中析出, 析出相显著球化细化, 尺寸约为 2 μm。经过对合金组织和力学性能的分析, 半固态挤压铸造 A356 合金的最佳热处理制度为: 540 °C 固溶 6 h, 180 °C 时效 4 h。经过固溶和时效处理后的合金抗拉强度达到 336 MPa, 延伸率达到 6.9%, 硬度达到 1240 MPa, 相较于热处理前的性能提升了 106.7%。

关键词: A356 合金; 半固态挤压铸造; 热处理; 微观组织; 力学性能

作者简介: 铁 镒, 男, 1983 年生, 博士, 副教授, 东北大学材料科学与工程学院, 辽宁 沈阳 110819, 电话: 024-83691463, E-mail: tie-di@hotmail.com